Original scientific paper
https://doi.org/10.33180/InfMIDEM2022.402

Informacije MIDEM
Journal of Microelectronics,
Electronic Components and Materials
Vol. 52, No. 4(2022), 215 – 226

Influence of Trace Eelements on the Electrical Properties of ZnO-based Multilayer Varistors

Slavko Bernik[1], Nana Brguljan[1], Marija Ercegovac[2], Zoran Samardžija[1]

[1]Department for Nanostructured Materials, Jožef Stefan Institute, Ljubljana, Slovenia
[2]Bourns, d.o.o., Žužemberk, Slovenia

Abstract: Nonlinear current-voltage (I-U) characteristics and stability after an I_{MAX} test of two types of multilayer varistors (MLVs), each type fabricated in two series, were analysed in terms of their structure, microstructure and the presence of trace (i.e., impurity) elements. The structural and microstructural features showed nothing significant that could justify the very different I_{MAX} characteristics of the MLVs of the same type from the two series. In the larger MLVs, declared for I_{MAX} 1000A, the most critical factor was found to be the amount of Fe, the source of which was the starting Cr_2O_3 powder; one batch of Cr_2O_3 used for their fabrication contained an about 5-times-larger amount of Fe than the other, while the amounts of the other impurity elements (i.e., Al, Si, Mg, Ca, Ti, Na, K) were similar in both. The MLV1000 samples prepared with the Fe-rich Cr_2O_3 powder failed after a current impulse of 900A, while the samples using the Fe-low Cr_2O_3 powder withstood even 1400A. In the smaller MLVs, declared for 200A, prepared from Fe-low Cr_2O_3 and added in half the amount as in the MLV1000 samples, the critical factor was the large addition of SiO_2 in the starting composition and the samples failed after a current impulse of 30 A. Amending the composition with the addition of several 100 ppm of Al resulted in an enhancement of I_{MAX} to 420A, demonstrating the positive effects of Al. The results indicated the need to control the presence of trace elements and showed the complexity of an issue that requires a thorough consideration for each type of MLV to achieve the required electrical characteristics.

Keywords: ZnO; multilayer varistors; trace elements; microstructure; electrical characteristics

Vpliv elementov v sledovih na električne lastnosti večplastnih varistorjev na osnovi ZnO

Izvleček: Nelinearne tokovno-napetostne (I-U) karakteristike in stabilnost po testu I_{MAX} dveh vrst večslojnih varistorjev (MLV), od katerih je bila vsaka izdelana v dveh serijah, smo analizirali glede na njihovo strukturo, mikrostrukturo in prisotnost elementov v sledovih (tj. nečistoč). Strukturne in mikrostrukturne značilnosti niso pokazale nič pomembnega, kar bi lahko pojasnilo zelo različne značilnosti I_{MAX} med MLV vzorci istega tipa iz obeh serij. Pri večjih MLV, deklariranih za I_{MAX} 1000A, se je izkazalo, da je najbolj kritičen dejavnik količina Fe, katerega vir je bil začetni prah Cr_2O_3; prah Cr_2O_3 ene serije, uporabljen za njihovo izdelavo, je vseboval približno 5-krat večjo količino Fe kot prah druge serije, medtem ko so bile količine ostalih nečistoč (tj. Al, Si, Mg, Ca, Ti, Na, K) v obeh podobne. Vzorci MLV1000, izdelani s prahom Cr_2O_3, bogatim s Fe, so odpovedali že po tokovnem impulzu 900 A, medtem ko so vzorci, pripravljeni s prahom Cr_2O_3 z malo Fe, zdržali celo 1400 A. Pri manjših MLV, deklariranih za 200 A, pripravljenih iz Cr_2O_3 z nižjo vsebnostjo Fe, ki je bil dodan v polovični količini kot pri vzorcih MLV1000, je bil kritičen dejavnik visok dodatek SiO_2 v začetni sestavi, tako da so vzorci odpovedali že po tokovnem impulzu 30 A. Sprememba sestave z dodatkom več 100 ppm Al je povzročila izboljšanje I_{MAX} na 420A, kar dokazuje pozitivne učinke Al. Rezultati so pokazali na pomembnost nadzora prisotnosti elementov v sledovih in na kompleksnost problematike, ki zahteva temeljit premislek za vsako vrsto MLV, da bi dosegli zahtevane električne karakteristike.

Ključne besede: ZnO; večplastni varistorji; nečistoče; mikrostruktura; električne lastnosti

** Corresponding Author's e-mail: slavko.bernik@ijs.si*

1 Introduction

Varistors, i.e., variable resistors are core elements of surge protection devices (SPDs), complying with a broad range of operating voltages for electrical devices and electronics, as well as for the stabilisation of low-, medium, and high-voltage electric power lines.

How to cite:
Slavko Bernik et al., "Influence of Trace Eelements on the Electrical Properties of ZnO-based Multilayer Varistors", Inf. Midem-J. Microelectron. Electron. Compon. Mater., Vol. 52, No. 4(2022), pp. 215–226

The varistors are made of ZnO-based varistor ceramics, which are characterised by an exceptional current-voltage (I-U) nonlinearity and a high energy-absorption capability. Accordingly, at the breakdown voltage the varistor switches from a highly resistive to a highly conductive state in a matter of nanoseconds and the current through the varistors increases by several orders of magnitude for a minimum change in voltage. Thus, a varistor connected in parallel effectively diverts the transient surge from the protected device to the ground and absorbs the excess harmful energy, ensuring the undisturbed and safe operation of the device, while preventing its damage or even destruction. The possibilities to tailor the break-down voltage of varistor ceramics from a few volts up to several kilo-volts enables suitable dimensions of varistors for applications across a broad range of voltages, a superior response time to transient surges, a high energy-absorption capability and a long-term operating stability and reliability. These advantages of varistors mean that they are effectively unmatched by any other surge-protection device. Hence, varistors dominate the worldwide, multi-billion euro business of overvoltage-protection applications [1-3].

The breakdown voltage of a varistor is proportional to the thickness of the ceramic and the energy-absorption capability is proportional to its volume. Hence, so-called bulk or disc varistors are predominantly used for medium- and high-voltage applications, which are also related to higher energies. For breakdown voltages below about 60V, thicknesses below 1 mm are required and the fabrication of such thin ceramic discs without any shape deformation during high-temperature sintering can be difficult, and there is a problem with their low fracture strength. With an increasing thickness-to-diameter ratio of the discs to increase their volume, and hence the energy-absorption capability, the problem of their low fracture strength further increases. The solution for low-voltage applications is multilayer varistors (MLV), which were developed in the 1980s as an answer to problems in low-voltage circuits, accompanied by a rapid trend for their miniaturisation and a constant demand for an enhanced integration scale in electronic circuits. The miniaturisation of electronic circuits increases their sensitivity to external interference and MLVs are used for low-voltage protection against transient surges caused by electrostatic discharge, atmospheric discharge and transient overvoltages generated for other reasons in integrated circuits, hybrid circuits and surface-mounted circuits [4-7]. Accordingly, MLVs also have key role in automotive-circuit protection as modern vehicles employ a variety of electronics for safety, assisted driving, self-driving, cameras, engine-performance optimisation with an engine-control unit, communications and navigation. Many of these systems require multiple processors as well as high-current sensors and actuators. Nowadays vehicles contain over 40 motors and actuators to drive windows, doors, seats, pumps, windshield wipers and other components. At the standard operating voltages of personal cars and trucks, i.e., 12V and 24V, respectively, the automotive MLVs with nominal voltages from 20 to 40V are exposed to extremely heavy loads that occur for instance when turning on or off the engine, or when any other power user is switched on (i.e., electrical adjustment of a seat, opening a window, etc.), which can cause transient voltage surges up to several 100 V lasting for several 100 ms and energy loads of more than 100 J. However, in hybrid electric vehicles using 48 V systems and plug-in electric cars using high-voltage systems (i.e., 400V and even higher) because the high voltage boosts efficiency and allows lower current for the same power (wattage), the requirements for MLVs are even greater. It should also be mentioned that MLVs have to show no deterioration in performance in the temperature range from – 55°C to 175°C. Accordingly, a great deal of attention has to be given to any detail of the fabrication technology for MLVs to comply with the rigorous performance requirements [8].

MLVs or "chip" varistors are composed from layers of fine-grained ZnO-based varistor ceramics with thicknesses typically in the range from 20 to 100 μm, internal electrodes connected in parallel and terminal outer electrodes, and are manufactured using multilayer fabrication technology. Flexible green ceramic tapes are prepared with tape-casting technology. Several green sheets with screen-printed inner electrodes (typically AgPd,) are stacked, isostatically laminated, diced into individual varistors, and co-sintered, typically at temperatures around 1000°C. The layers are laminated in a way that the inner electrodes form alternating connections between the two terminal electrodes; accordingly, every other layer connects to the same terminal electrode. Such a configuration allows for higher resistances at lower voltages with faster response times than the bulk metal oxide varistors (MOV). Basically, the breakdown or nominal voltage of MLVs is determined by the thickness of the ceramic layer between the two inner electrodes, while their energy-absorption capability can be adjusted with the number of layers (i.e., the thickness of MLV) and the area of MLV, i.e., by adjusting its volume [5, 9].

Among the generally well-known types of the ZnO-based varistor ceramics, i.e., ZnO-Bi_2O_3-based, ZnO-Pr_6O_{11}-bazed, and ZnO-V_2O_5-based, the ZnO-Bi_2O_3-based ones are the most widely used for bulk varistors and MLVs. ZnO is an n-type, wide-band-gap semiconductor. The current-voltage (I-U) nonlinearity, which is typically described with the expression (0)

$$I = kU^{a} \quad (0)$$

(k – constant, α – coefficient of nonlinearity), is induced to ZnO by the addition of varistor formers like Bi_2O_3; it segregates at the ZnO grain boundaries and results in the formation of electrostatic Schottky barriers so that the non-ohmic (i.e., varistor) grain boundary has a breakdown voltage U_{GB} of about 3.2V. Varistor formers facilitate the formation of acceptor states at the grain boundaries, i.e., oxygen interstitials (O_i'') and zinc vacancies (V_{Zn}', V_{Zn}''), which act as electron traps, while in the vicinity of grain boundaries, in the ZnO grain, a positively charged depletion layer of oxygen vacancies ($V_O^{\cdot}$, $V_O^{\cdot\cdot}$) and zinc interstitials ($Zn_i^{\cdot}$, $Zn_i^{\cdot\cdot}$) is formed. The weak nonlinearity of Bi_2O_3-doped ZnO with α of about 3 is further enhanced by the addition of dopants like Sb_2O_3, Co_3O_4, Mn_3O_4, NiO and Cr_2O_3 to values of α from 20 to 80. While some of these dopants are essential to increase the electrical conductivity of the ZnO grains (Co, Mn, Ni), the other (Sb, Cr) affect the growth of the ZnO grains and thus enable tailoring of the breakdown voltage (U_B) of varistor ceramics via grain size (G) in accordance with the expression (1)

$$U_B = \frac{U_{GB} * t}{G} = U_{GB} * N_{GB} \quad (1)$$

where *t* is thickness of ceramics and N_{GB} number of grain boundaries. Although the varistor dopants added to ZnO typically account in total for less than 10 wt.%, such a composition results in a rather complex microstructure of the varistor ceramics. It contains the ZnO phase and secondary phases of the ZnO-Bi_2O_3-Sb_2O_3 system, i.e., a Bi_2O_3-rich phase, a $Zn_7Sb_2O_{12}$-type spinel phase and a $Bi_3Zn_2Sb_3O_{14}$-type pyrochlore phase, while the other varistor dopants (i.e., Co, Mn, Ni, Cr) are incorporated into these phases. The electrical characteristics of the varistor ceramics, i.e., breakdown voltage (U_B), coefficient of nonlinearity (α) and leakage current (I_L), are primarily affected by the ZnO phase, which must be highly conductive, and the Bi_2O_3-rich phase at the grain boundaries for their non-ohmic varistor characteristic (highly resistive at voltages below U_B). It is also important that the Bi_2O_3 forms a liquid phase during sintering and, besides the ZnO, dissolves all the other varistor dopants, thus greatly affecting their distribution in the microstructure as well as the sintering and the grain-growth process. Accordingly, all the dopants in equilibrium amounts are incorporated into the Bi_2O_3-rich phase, thus affecting the electronic states at the grain boundaries and consequently also their electrical characteristics [1, 2, 6, 7].

Some elements can greatly affect the electrical characteristics of the varistor ceramics in very small amounts of up to only several 100ppm. They can act as donors, acceptors, or both, depending on the nature, concentration and location in the host crystal lattice. In the microstructure they can be grain boundary or grain specific and accordingly they affect the current-voltage (I-U) characteristics in the "pre-breakdown" region at low currents or in the "upturn" region at high currents, or both. The controlled addition of such carefully selected elements can be used for a targeted improvement of the electrical and energy characteristics of varistor ceramics. For example, fine doping with Al is generally used for the enhanced stability of varistor ceramics at high currents due to the improved electrical conductivity of the ZnO grains; however, it also increases the leakage current. In contrast, the fine addition of Si increases the resistivity of the grain boundaries, thus it is often used to decrease the leakage current of varistor ceramics. Unfortunately, elements that strongly affect the functional properties of varistor ceramics, even in very small quantities, can also be added unintentionally as impurities of the standard varistor dopants, which represents a serious problem. Hence, it is important to control the presence of impurity elements in the oxide powders used for the fabrication of varistor ceramics [10-12].

In this work two types of the multilayer varistors (MLV) from two fabrication series were analysed and their current-voltage (I-U) and energy characteristics are discussed in terms of their structure, microstructure and the presence of impurity (i.e., trace) elements, the primary source of which was confirmed to be the starting Cr_2O_3 powder. In the larger type of MLVs, used for maximum current impulses of I_{MAX}=1000A, the most critical for the stability against high current impulses was the amount of Fe impurity present. At a much lower amount of Fe (< 10 ppm) and a similar amount of other impurities (i.e., Al, Si, Mg, Ca, Ti, Na, K) the characteristics of this type of MLV were excellent with an I_{MAX} of 1400A, while MLVs prepared from Fe-rich Cr_2O_3 and thus containing about 40 ppm of Fe failed at current impulses of 900A. In the case of smaller MLVs, declared for I_{MAX}=200A, too much SiO_2 added in the starting composition was found to be critical and they failed at 30A. However, amending their starting composition with the addition of Al resulted in significantly improved energy characteristics, raising their I_{MAX} to 420A. The results indicated the importance of controlling the presence of trace elements, which can critically affect the performance of MLVs.

2 Materials and methods

Two types of MLVs, i.e., the larger, declared for a maximum impulse current (I_{MAX}) of 1000A (labelled MLV1000) and the smaller, declared for an I_{MAX} of 200A (labelled

MLV200), were prepared with standard multilayer fabrication technology in the Bourns company [4, 13]. In all the MLVs the same reagent grade powders of oxides of Zn, Bi, Sb, Co, Mn, Cr and Si were used; however, in the case of Cr_2O_3, powders from the same producer but from two different batches were used, both having the same composition according to the supplier, and are here labelled Cr1 and Cr2. For the MLV1000, ceramic tapes with the composition 97.9ZnO + 2.1(Bi_2O_3, Sb_2O_3, Co_3O_4, Mn_3O_4, Cr_2O_3) were used. One series of this type was prepared from tapes with Cr1 (series MLV1000-Cr1) and the other series from ceramic tapes with Cr2 (series MLV1000-Cr2). The smaller MLVs were prepared from ceramic tapes with the composition 98.0ZnO + 2.0(Bi_2O_3, Sb_2O_3, Co_3O_4, Mn_3O_4, Cr_2O_3, SiO_2); in one series the tapes containing Cr2 (series MLV200-Cr2) and in the other series the ceramic tapes also contained Cr2 but with their composition altered with addition of several 100 ppm of Al as solution of $Al(NO_3)_3 \cdot 9H_2O$ (series MLV200-Cr2Al). It should be mentioned that in the MLV1000 the amount of added Cr_2O_3 was twice the amount added in the MLV200. In the MLV200 samples, however, also a large amount of about 0.1mol.% of SiO_2 was added to the starting composition of the ceramic tapes, which was not added to the MLV1000. All the series of MLVs were co-sintered with AgPd electrodes in air at about 1000°C for the same duration, the series MLV200 at about 20 to 30°C lower temperature than the series of MLV1000 samples.

The current-voltage (I-U) characteristics of the MLV samples were measured using a Keithley 2410 Source Meter, i.e., nominal voltage (i.e., breakdown voltage), U_N, was determined at a current of 1 mA, leakage current, I_L, at $0.75U_N$, and the coefficient of nonlinearity, α, was determined in accordance with the equation (2)

$$a = \frac{\log\left(\frac{I_2}{I_1}\right)}{l\log\left(\frac{U_2}{U_1}\right)} \quad (2)$$

where U2 and U1 are voltages measured at I1 = 1 mA and I2 = 10 mA, respectively. The high current stability was determined by the maximum impulse current (I_{MAX}) at which the U_N of the MLVs changes by less than 10%. The I_{MAX} of the samples was analysed using an AMC MIG0606 impulse generator with current impulses of shape 8/20 (i.e., rising time 8 μs, duration 20 μs) to simulate impulses caused by a lightning strike) at current intensities from 200A to 500A for series MLV200 and from 900A to 1500A for series MLV1000. The I-U characteristics of the samples were measured before and after the current impulse test and their average values determined based on measurements of at least 10 samples per test.

Microstructures in the cross-section of the MLVs, perpendicular to the plane of the internal electrodes, were prepared and analysed in the scanning electron microscope (SEM) JEOL JSM-7600F equipped with an energy-dispersive spectrometer (EDS) Oxford Instruments INCA. The integrity of the inner electrodes, the distance between them and their connectivity to the terminal electrodes was examined. Also, the microstructure of the varistor ceramics was analysed with regard to the phase composition, phase homogeneity of the microstructure, porosity, grain size and grain size distribution. The phase composition of the ceramics was also determined with a powder x-ray diffraction analysis (XRD).

Furthermore, starting oxide powders used for the preparation of the foils of varistor ceramic using tape-casting technology were examined for their crystal structure (XRD), grain size and grain size distribution (particle size analyser HORIBA), morphology of the particles (SEM analysis), and the chemical composition (SEM/EDS). Finally, for all the used oxide powders, a precise quantitative analysis of the trace impurity elements was also made using the inductively coupled plasma - optical emission spectrometry method (ICP-OES).

3 Results and discussion

The average current-voltage (I-U) characteristics of the MLV1000 samples before and after the I_{MAX} current impulse test are presented in Tables 1 and 2. For this type of MLV an I_{MAX} of at least 1000A is required, and as can be seen in Table 1 none of the MLV samples from the series MLV1000-Cr1 complied with this requirement. In the first line of the table (i.e., shaded grey) the average I-U characteristics of all the MLV samples from this series measured before the I_{MAX} test are given. In comparison to these reference values, already after current impulse of 900A the I-U characteristics deteriorated, as indicated by a decrease of the nominal voltage (U_N) and the coefficient of nonlinearity (α), while the leakage current (I_L) significantly increased. The degradation of the I-U characteristics of the MLVs from this series further increased with a rising of the current impulse's intensity so that after an impulse of 1200A the average U_N decreased by 34 %, the α decreased by 50% from 34 to 17, and the I_L increased strongly. In contrast, the samples from the series MLV1000-Cr2 (Table 2) showed excellent stability even after current impulses of 1300A and 1400A, and failed only after tests at 1500A.

Table 1: Current-voltage characteristics (I-U) of MLV1000 samples from series MLV1000-Cr1 before and after I_{MAX} test.

I_{MAX} /A	U_N/V (±σ/%)	α (±σ/%)	I_L/μA (±σ/%)	ΔU_N /%
Ref.	35.1 (3)	34 (6)	1.6 (70)	/
900	29.1 (54)	25 (57)	201 (223)	-17
1000	30.5 (38)	22 (61)	202 (221)	-13
1100	24.3 (61)	16 (89)	403 (135)	-30
1200	23.0 (74)	17 (88)	438 (119)	-34

Such drastically different I_{MAX} characteristics between the MLV1000 samples from two series could result from some failure in their fabrication, which would show in their microstructure. Accordingly, their microstructures were examined for possible defects to the internal electrodes, like not being whole or continuous, but with interruptions, uniformity of the distance between internal electrodes, number of internal electrodes, poor or failed connection of the internal electrodes with terminal electrodes, and also in regard to the microstructure and phase composition of the varistor ceramics. The microstructures of several MLV1000 samples from each series were examined on the SEM and nothing significant that could explain the different electrical characteristics was found. Typical microstructures of the MLV1000 samples in the cross-section direction are presented in Fig. 1.

Table 2: Current-voltage characteristics (I-U) of MLV1000 samples from series MLV1000-Cr_2 before and after I_{MAX} test.

I_{MAX} /A	U_N/V (±σ/%)	α (±σ/%)	I_L/μA (±σ/%)	ΔU_N /%
Ref.	33.0 (2)	33 (4)	1.4 (36)	/
1300	32.9 (4)	32 (4)	2.9 (70)	1
1400	33.4 (1)	32 (3)	3.9 (54)	1
1500	24.6 (58)	20 (81)	402 (136)	-27

The internal electrodes, 7 in total, were found in all the analysed samples from both series to be continuous, at a uniform distance of about 104 μm, and all well in contact with the terminal electrodes. Also, the SEM analysis of the varistor ceramics showed no difference in the microstructure of the MLV1000 samples from both series in terms of porosity, phase composition and homogeneity in the distribution of secondary phases among the ZnO grains. In all the samples, besides the matrix ZnO phase, also a secondary Bi_2O_3-rich liquid phase, a $Zn_7Sb_2O_{12}$-type spinel phase, and a $Bi_3Zn_2Sb_3O_{14}$-type pyrochlore phase were determined by the EDS analysis. In Fig. 2, typical microstructures and phase compositions of the samples MLV1000-Cr1

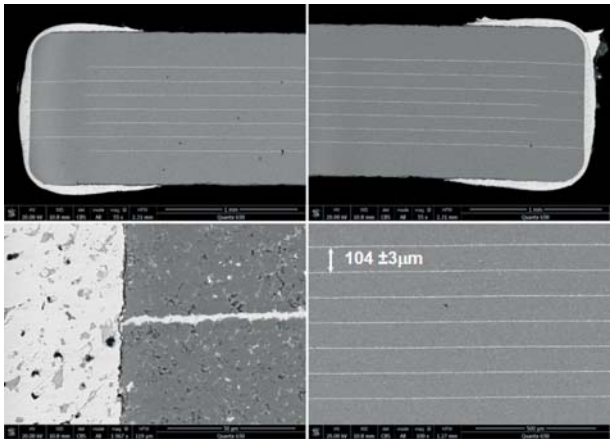

Figure 1: Typical microstructure of MLV1000 samples in cross-section showing internal electrodes and their connection to the terminal electrodes.

(2.a-b) and MLV1000-Cr2 (1.c-d) are shown. SEM analysis of the etched microstructures (Fig. 3) showed that the samples MLV1000 from both series also have similar ZnO grain sizes and size distributions (Fig. 3).

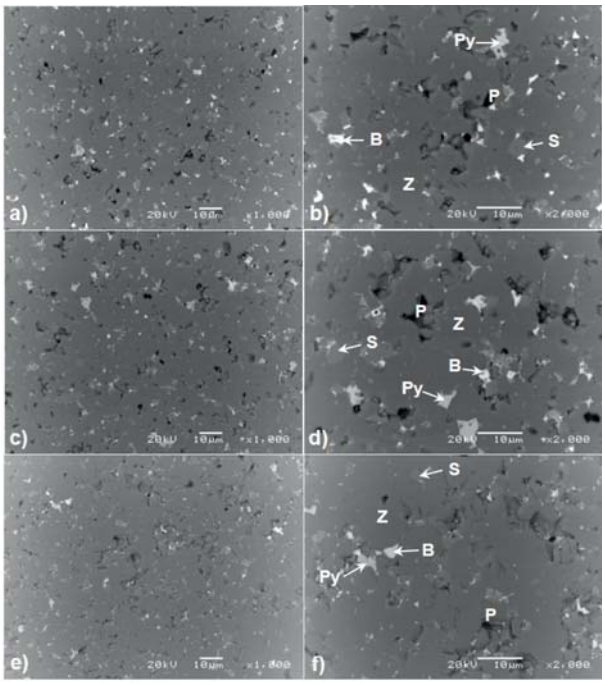

Figure 2: SEM images in backscattered mode (BE) of the microstructures of the MLV samples; (a,b) MLV1000-Cr1, (c,d) MLV1000-Cr2, and (e,f) MLV200-Cr2. Phase labelling: Z – ZnO phase, B – Bi_2O_3-rich phase, Py – $Bi_3Zn_2Sb_3O_{14}$-type pyrochlore phase, S – $Zn_7Sb_2O_{12}$-type phase, P – pore.

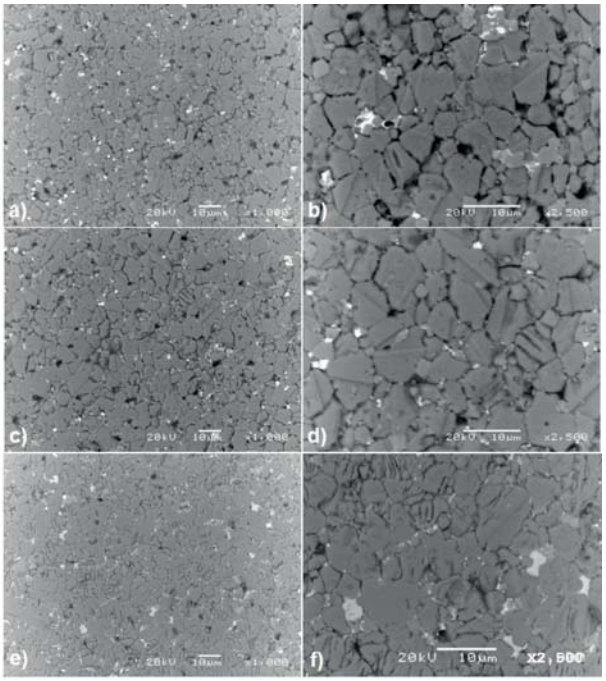

Figure 3: SEM/BE images of the etched microstructures of the MLV samples; (a,b) MLV1000-Cr1, (c,d) MLV1000-Cr2, and (e,f) MLV200-Cr2.

The XRD analysis also confirmed the same phase composition of the MLV1000 samples from both series, showing besides the ZnO phase also a Bi_2O_3-rich liquid phase as a γ-Bi_2O_3 modification and a $Zn_7Sb_2O_{12}$-type spinel phase. The XRD peaks of the $Bi_3Zn_2Sb_3O_{14}$-type pyrochlore phase, which was found by the SEM/EDS analysis in the microstructures of the MLV1000 samples, strongly overlap with the other phases present. Hence, it is difficult to detect pyrochlore phase in the varistor ceramics by the XRD analysis. The typical XRD pattern of the varistor ceramics in the analysed MLV samples is shown in Fig. 4.

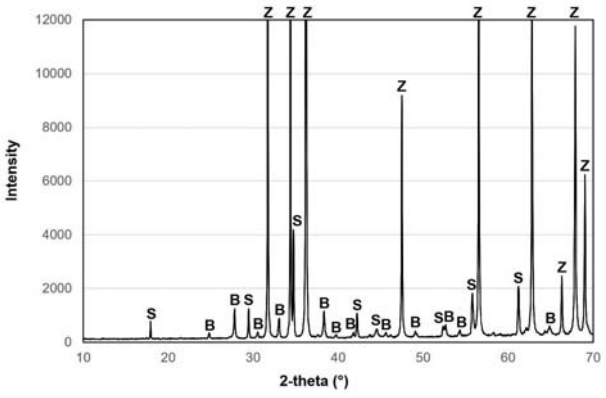

Figure 4: Typical XRD pattern of the varistor ceramics in the analysed MLV samples. Phase labelling: Z – ZnO phase, B – γ-Bi_2O_3 phase, S - $Zn_7Sb_2O_{12}$-type phase.

The average I-U characteristics of the smaller MLV200 samples before (i.e., reference values) and after the current impulse test are given in Tables 3 and 4. The samples of the series MLV200-Cr2 showed extremely poor I_{MAX} characteristics (Table 3); while they should withstand a current impulse of 200A with a change in the U_N of less than 10% at a preserved coefficient of nonlinearity (α) and a low leakage current (I_L), even a current impulse of just 30A resulted in a significant decrease of U_N by 18%, accompanied with a decrease in α and a significant increase in I_L.

Table 3: Current-voltage characteristics (I-U) of the MLV200 samples from the series MLV200-Cr2 before (reference values) and after I_{MAX} test.

I_{MAX} /A	U_N/V (±σ/%)	α (±σ/%)	I_L/µA (±σ/%)	ΔU_N /%
Ref.	28.1 (3)	29 (6)	0.2 (106)	/
30	23.0 (53)	24 (53)	200 (224)	-18
50	23.4 (51)	24 (53)	200 (224)	-17
100	12.9 (61)	13 (121)	600 (91)	-30

The samples from the series MLV200-Cr2Al (Table 4), however, showed excellent stability for current impulses, even up to 420A, while after a load with 440 A their I-U characteristics significantly decreased and even more after a current impulse of 500A.

Table 4: Current-voltage characteristics (I-U) of the MLV200 samples from the series MLV200-Cr2Al before (reference values) and after I_{MAX} test.

I_{MAX} /A	U_N/V (±σ/%)	α (±σ/%)	I_L/µA (±σ/%)	ΔU_N /%
Ref.	26.9 (4)	32 (8)	1.5 (109)	/
200	28.1 (2)	33 (10)	0.6 (24)	1
260	28.7 (2)	31 (9)	0.4 (28)	1
300	27.1 (4)	31 (8)	1.5 (121)	1
340	27.1 (3)	31 (19)	1.4 (11)	1
380	26.5 (3)	26 (14)	1.7 (38)	2
400	26.7 (2)	28 (31)	1.9 (68)	2
420	26.8 (1)	30 (4)	2.3 (31)	1
440	19.4 (56)	18 (80)	402 (136)	-27
500	11.5 (119)	10 (121)	647 (76)	-56

Microstructural analysis of the MLV200 samples from both series showed that all six internal electrodes have a similar thickness and are continuous, even at a distance of about 80 µm, and well connected to the terminal electrodes (Fig. 5). Also, the SEM/EDS analysis of the varistor ceramics showed similar microstructures in terms of the phase composition and the grain size (Figs. 2.e-f, and 3.e-f). The same phase composition of

the varistor ceramics in the MLV200 samples from both series was also confirmed by the XRD analysis (Fig. 4).

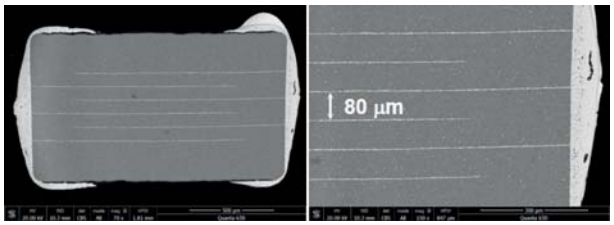

Figure 5: SEM/BE images showing typical cross-section microstructure of the samples MLV200.

The results showed that in both types of MLVs, the MLV1000 and MLV200 of both series, varistor ceramics have similar microstructures and phase compositions according to the SEM/EDS and XRD analysis. Actually, these analyses revealed nothing related to the microstructure of the ceramics and the structure of the MLVs, including possible technical errors in their fabrication, that could explain such drastically different stabilities in the I-U characteristics after the current impulse tests (IMAX test) between the same type of MLVs from two fabrication series. However, such results indicated that attention should be given to know the differences in the preparation of the MLV samples, i.e., in the case of the MLV1000 samples the use of Cr_2O_3 from different batches and in the case of MLV200 samples an alteration of the composition with the addition of Al in one fabrication series as compared to the other, while in both the Fe-low Cr_2O_3 from the same batch was used. Accordingly, the Cr_2O_3 powders used for the preparation of the MLV samples were thoroughly analysed.

Granulometric analyses of the Cr_2O_3 powders from both batches showed that they have similar average particle sizes of about 2.1 μm and also similar particle size distributions in the range from 0.2 μm to 10 μm, as shown in Fig. 6. The typical morphology of the used Cr_2O_3 powders is shown in Fig. 7 and compliments the results of the granulometric analysis.

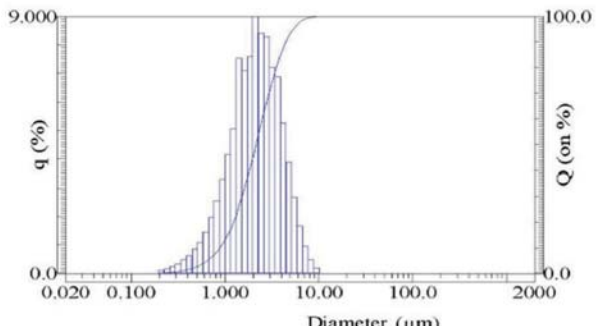

Figure 6: Histogram of the particle size distribution in the Cr_2O_3 powder.

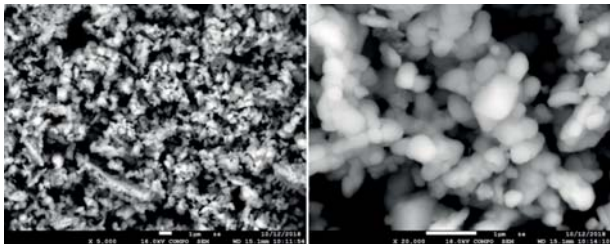

Figure 7: SEM images showing typical morphology of the Cr_2O_3 powders used for the fabrication of the MLV samples.

The XRD patterns of both powders are very similar (Fig. 8) and can be identified using the reference pattern for Cr_2O_3 JCPDF 00-038-1479. However, in the Cr1 powder additional minor peaks indicate the presence of some SiO_2 secondary phase (JCPDF01-082-1556).

Detailed SEM/EDS analyses revealed, in both Cr_2O_3 powders, the presence of a significant amount of secondary phases as coarse-grained inclusions containing impurity elements, primarily Si, Al and Fe, and also K, Na, Ca and Ti (Fig. 9). Hence, a quantitative chemical ICP-OES analysis was made to determine the content of trace impurity elements in the Cr_2O_3 powders. The results of the ICP-OES analysis of the Cr_2O_3 from both batches are presented in Table 5.

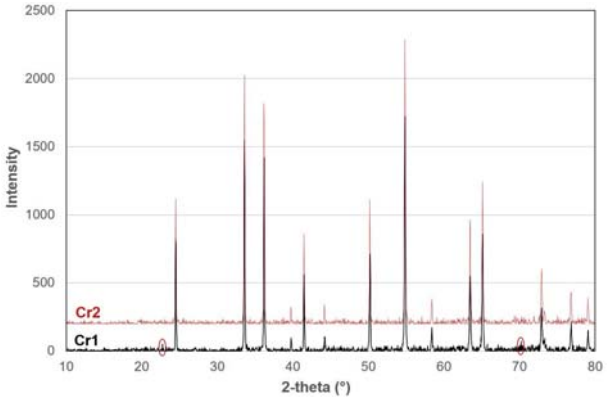

Figure 8: XRD patterns of the Cr_2O_3 powders; in the Cr1, additional to the peaks of Cr_2O_3, also additional minor peaks indicate the presence of the SiO_2 secondary phase.

The quantitative ICP-OES analysis of all the other oxides used for the fabrication of the studied MLV samples (i.e., ZnO, Sb_2O_3, Co_3O_4, and Mn_3O_4) showed the presence of the impurity elements below 50 ppm, confirming that the main source of impurities is Cr_2O_3.

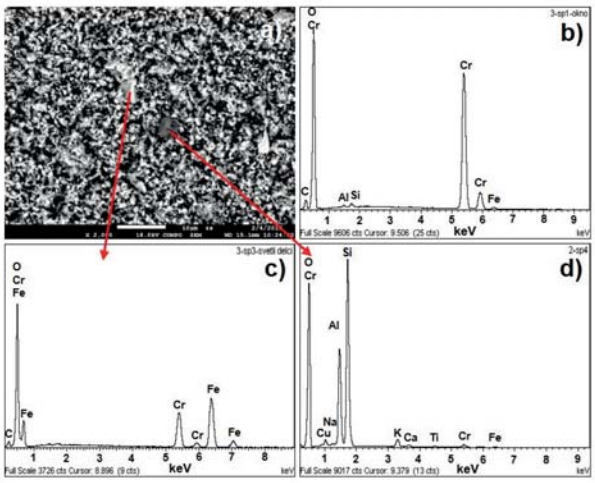

Figure 9: a) SEM/BE image of the Cr_2O_3 powder Cr1, b) EDS analysis of area on SEM image, c) point EDS analysis of lighter secondary phase, and d) points EDS analyses of darker secondary phase.

Table 5: Results of the quantitative ICP-OES analysis of the used Cr_2O_3 powders, i.e., Cr1 and Cr2, for the amount of impurity elements.

Composition	Cr_2O_3 powder	
M(ppm)/MO(wt.%)	Cr1	Cr2
Cr_2O_3	97.08	97.99
Si/SiO_2	10080/1.57	10020/1.49
Al/Al_2O_3	3502/0.12	2801/0.10
Fe/Fe_2O_3	9488/0.92	1944/0.19
Mg/MgO	932/0.10	779/0.09
Ca/CaO	888/0.08	797/0.08
Ti/TiO_2	172/0.02	127/0.01
Na/Na_2O	477/0.04	231/0.02
K/K_2O	870/0.07	351/0.03

These results showed the contamination of both Cr_2O_3 powders used in the preparation of the MLVs, with numerous impurity elements that are known to have an influence on the current-voltage (I-U) characteristics and the stability of the varistor ceramics. Several models are proposed, explaining the voltage stability/instability of the ZnO-based varistor ceramic through the degradation of the electrostatic barriers at the grain boundaries. However, it is common to most of them that the origin of the degradation is assigned to the diffusion of zinc interstitials (Zn_i) from the depletion layer and their chemical interaction with acceptor states at the grain boundaries, i.e., oxygen interstitials (O_i) and zinc vacancies (V_{Zn}), which consequently leads to the degradation and collapse of the electrostatic Schottky barriers [1, 10, 11, 14-16]. Their degradation is typically expressed by a decrease in the nominal (i.e., breakdown) voltage of the varistor ceramics (U_N) due to the reduced breakdown voltage of the grain boundaries (U_{GB}), a decrease in the coefficient of nonlinearity (α) and a significant increase of the leakage current (I_L), as observed in the case of the poor MLVs in this work. Actually, most of the impurity elements detected in the Cr_2O_3 are reported in the literature as having a positive influence in low amounts and some of them are even known as "varistor highlighters", like Al and Si, which are intentionally added to the starting composition in ppm amounts to enhance the performance of the varistor ceramics in the low-current pre-breakdown region or in the high-current "up-turn" region of their I-U curve [2]. They affect the defect equilibria and electronic states at the grain boundaries, and thus the height and stability of the electrostatic Schottky barriers at the grain boundaries, which are responsible for the I-U nonlinearity of varistor ceramics. On the other hand, they can increase the electrical conductivity of the ZnO grains, which has a positive influence on the stability and aging characteristics of varistor ceramics due to lowering the released Ohmic heat under high current loads [1, 10].

The main impurity detected in Cr_2O_3 powders is certainly Si (i.e. SiO_2), as can be seen in Table 5. Studies showed that SiO_2 in low amounts strongly affects the electronic states at the grain boundaries, resulting in an increase of the height of the electronic Schottky barriers and also the coefficient of nonlinearity (α). Also, the increased resistivity of the grain boundaries results in a lower leakage current (I_L). At the same time, SiO_2 also increases the depletion-layer width, leading to the enhancement of the breakdown voltage of the grain boundaries (U_{GB}). However, too much Cr_2O_3 could result in a deterioration of the I-U characteristics, especially once the secondary Zn_2SiO_4 phase starts to form at the grain boundaries [12, 17, 18]. Another impurity element detected in the Cr_2O_3 powders in amounts of several 1000ppm is Al; it is often considered at the main "varistor highlighter" and also generally known as the main donor dopant in ZnO-based ceramics. Numerous studies showed that it enhances the energy stability of the ZnO-based varistor ceramics when added in amounts of several 100 ppm, by increasing the conductivity of the ZnO grains. However, Al is not a grain selective dopant, but also influences the electronic states at the grain boundaries, resulting in an increase of the leakage current (I_L). Also, at higher amounts of Al, which depends on the sintering temperature and time, it starts to incorporate at the interstitial sites in the crystal structure of ZnO, acting as an acceptor and decreasing the conductivity of the ZnO grains. Hence, thorough control of the amount of Al is required, depending on the sintering conditions [11, 19-22]. The amphoteric dopants in ZnO are Na and K. In very low amounts of a few 10 ppm, Na (and K) incorporate at the

interstitial sites of the ZnO crystal lattice and act as donors, increasing the electrical conductivity of the ZnO grains, while at the same time they substitute for the interstitial Zn (Zn_i) in the depletion layer, decreasing its concentration and thus increasing the stability of ZnO varistor ceramics. However, in larger amounts, Na (K) incorporates at the regular sites of Zn in the structure of ZnO (Na_{Zn}') and acts as an acceptor, decreasing the electrical conductivity of the ZnO grains [10, 23, 24]. The positive influence of low levels of doping was also reported for Mg [24, 25] and Ca [24, 26-28]; both of them result in a decrease of the leakage current (I_L), an increase of the breakdown voltage (U_B) and an increase of the coefficient of nonlinearity (α). In the case of Ca it has been reported that it increases the solid solubility of Al in the ZnO, thus enhancing the electrical conductivity of the ZnO grains, while reducing the accumulation of Al at the grain boundaries, which increases their resistivity [28]. If added in too large amounts, each of them results in secondary phases at the grain boundaries of the ZnO, causing deterioration of the I-U characteristics of varistor ceramics; in the case of Mg the Mg-Zn-O periclase solid solution is formed [25], and in the case of Ca the Ca-Bi-O phases [26]. In contrast to other impurity elements found in Cr_2O_3, which have a positive influence, Fe has a negative influence on the I-U characteristics of the varistor ceramics already in low amounts [29-32], decreasing the breakdown voltage (U_B) and the coefficient of nonlinearity (α), and increasing the leakage current (I_L). Peiteado et al. [30] explained such influence of Fe by its incorporation into the $Zn_7Sb_2O_{12}$-type spinel phase at the grain boundaries, which strongly increases the electrical conductivity of otherwise insulating secondary phase, and thus increases the conductivity of varistor ceramics below the breakdown voltage, enhancing their electrical degradation.

Some of the impurity elements are present in the Cr_2O_3 powders in significant amounts of several 1000 ppm, and if present in such amounts in the varistor ceramics, they would likely have a negative influence on the I-U characteristics. However, for the amounts of Cr_2O_3 in the composition of the varistor ceramics, 1000 ppm of the impurity element in Cr_2O_3 means about 4 ppm in the varistor ceramics. Accordingly, most of the impurity elements, which are introduced by Cr_2O_3 into the varistor ceramics of the studied MLV samples, are present in very low amounts. This can have a positive influence on their I-U characteristics, if any. Only Fe is known to have a negative influence and in the I-U characteristics of varistor ceramics, even in very small amounts. In the samples from the series MLV1000-Cr1, the Fe is present in the amount of almost 40 ppm and in the same type MLV samples from the series MLV1000-Cr2 only in the amount of about 8 ppm. Accordingly, too much Fe in the MLV1000-Cr1 samples is the likely reason for their poor I_{MAX} characteristic, when they failed at a current impulse of 900A (Table 1). In the samples MLV1000-Cr2, however, the amount of Fe is below some critical value; therefore, they can have an excellent I_{MAX} of 1400A (Table 2).

In the smaller MLV200 samples, the amount of added Cr_2O_3 is half the amount added in the samples MLV1000-Cr_2. Hence, the amount of impurity elements in the varistor ceramics of MLV200 samples is even lower, only about 2 ppm for 1000 ppm present in Cr_2O_3. Accordingly, impurity elements probably have even less influence on the I-U characteristics of the MLV200 samples than on the MLV1000-Cr2 samples, but in the case of most of them, it is likely a positive one. This indicates that the poor I_{MAX} characteristics of the sample from the MLV200-Cr2 series (Table 3) is likely caused by too much SiO_2 in the starting composition of the varistor ceramics. However, the much better performance of the samples from the series MLV200-Cr2Al (Table 4), having the starting composition of the varistor ceramics corrected with the addition of Al in the optimal amount of several 100 ppm, indicates the positive effect of Al, compensating the negative effect of the excess Si, and thus increasing the I_{MAX} to even 420A.

4 Conclusions

Two types of ZnO-Bi_2O_3-based multilayer varistors (MLVs), declared for different maximum current impulses (I_{MAX}), were studied. Their current-voltage (I-U) and energy characteristics (I_{MAX} test with current impulses 8/20) were analysed in terms of their structure, microstructure, starting composition and presence of the impurity (i.e., trace) elements.

The larger MLV samples, declared for the I_{MAX} 1000A (MLV1000), which were fabricated in two series using Cr_2O_3 from different batches, showed dramatically different current-voltage (I-U) characteristics after I_{MAX} tests. The samples MLV1000 from one series failed already after a current impulse of 900A, while the samples from the other series preserved the I-U characteristics even after a load with a current impulse of 1400A. Detailed analysis of their microstructure, phase composition and internal structure showed nothing significant that could explain such large differences in I_{MAX} between the MLV1000 samples from both series. The compositional analysis showed that the used Cr_2O_3 powders contained a number of impurity elements in amounts from several 1000 ppm (Al, Fe) to even 10,000 ppm (Si), and from a few 100 ppm to 1000 ppm (Mg, Ca, Ti, Na, K). While the amount of most impurity elements was similar in the Cr_2O_3 powders from both series,

the amount of Fe in one powder was almost 5 times higher (9500 ppm) than in the other (1950 ppm). For the amount of Cr_2O_3 in the composition of varistor ceramics, 1000 ppm of the impurity element in the Cr_2O_3 means about 4 ppm in the varistor ceramics. Most of these elements are known to enhance the nonlinear I-U characteristics and the stability of the ZnO-Bi_2O_3-based varistor ceramics when present in such low amounts as introduced by the Cr_2O_3. The exception is Fe, which is known to degrade the I-U characteristics already for very small amounts. The difference in the I_{MAX} of the MLV1000 samples from the two series can be attributed to different content of Fe. In the poor series of MLV1000 samples, the Fe-rich Cr_2O_3 powder resulted in almost 40 ppm of Fe in the varistor ceramics and consequently a degradation of their I-U characteristics even for current impulses below the declared 1000A. For comparison, in the good MLV1000 series, the Fe-low Cr_2O_3 powder introduced less than 10 ppm of Fe to the varistor ceramics.

In the case of smaller MLVs, declared for 200A, with the Fe-low Cr_2O_3 added in half the amount as in the samples MLV1000 and with addition of SiO_2, also significant differences in I_{MAX} characteristics were observed between the two fabrication series, one with and one without the addition of Al. The samples from the series without added Al failed already after a current impulse of 30 A. In contrast, the samples from the other series having a starting composition of the varistor ceramics amended with the addition of several 100ppm of Al endured current impulses with the shape 8/20 even up to 420A without changes in their I-U characteristics and failed only at higher current impulses. Such results indicated that the addition of Al neutralized the negative effect of the too large amount of added SiO_2 and significantly improved the I_{MAX} characteristics of the MLV200 samples.

The results show the importance of controlling the presence of trace elements, the source of which can be the starting raw materials for the preparation of varistor ceramics, or they could be intentionally added in the starting composition, as well as understanding their influence so as to achieve the required MLV properties.

5 Acknowledgments

This work was supported by the European Regional Development Fund and Ministry of Education, Science and Sport of Republic of Slovenia (Project Grants C3330-18-952024).

6 Conflict of Interest

The authors declare no conflict of interest in connection to the work presented.

7 References

1. D. R. Clarke, "Varistor ceramics," *Journal of the American Ceramic Society,* vol. 82, no. 3, pp. 485 - 502, 1999.
2. T. K. Gupta, "Application of zinc oxide varistors," *Journal of the American Ceramic Society,* vol. 73, no. 7, pp. 1817-1840, 1990.
3. "Global Metal Oxide Varistor Market Size - Global Industry Size, Share, Trends, Competitions and Forecast, 2017-2022," 2022.doi: https://www.techsciresearch.com/report/metal-oxide-varistor-market/3674.html
4. D. Szwagierczak, J. Kulawik, and A. Skwarek, "Influence of processing on microstructure and electrical characteristics of multilayer varistors," *Journal of Advanced Ceramics,* vol. 8, no. 3, pp. 408-417, 2019. https://doi.org/10.1007/s40145-019-0323-7
5. L. Wang, G. Tang, and Z.-K. Xu, "Preparation and electrical properties of multilayer ZnO varistors with water-based tape casting," *Ceramics International,* vol. 35, no. 1, pp. 487-492, 2009. https://doi.org/10.1016/j.ceramint.2008.01.011
6. W.-H. Lee, W.-T. Chen, Y.-C. Lee, S.-P. Lin, and T. Yang, "Relationship between Microstructure and Electrical Properties of ZnO-based Multilayer Varistor," *Japanese Journal of Applied Physics,* vol. 45, no. 6A, pp. 5126-5131, 2006. https://doi.org/10.1143/jjap.45.5126
7. S. Hirose, K. Nishita, and H. Niimi, "Influence of distribution of additives on electrical potential barrier at grain boundaries in ZnO-based multilayered chip varistor," *Journal of Applied Physics,* vol. 100, no. 8, 2006. https://doi.org/10.1063/1.2358833
8. (2019). *Multilayer varistors in automotive circuit protection*. Available: https://electronics360.globalspec.com/article/14398/multilayer-varistors-in-automotive-circuit-protection
9. J. Kulawik, D. Szwagierczak, and A. Skwarek, "Electrical and microstructural characterization of doped ZnO based multilayer varistors," *Microelectronics International,* vol. 34, no. 3, pp. 116-120, 2017. https://doi.org/10.1108/mi-02-2017-0009
10. T. K. Gupta and A. C. Miller, "Improved stability of the ZnO varistor via donor and acceptor doping

at the grain boiundary," *Journal of Material Research,* vol. 3, no. 4, pp. 745-751, 1988.
11. T. K. Gupta, "Microstructural engineering through donor and acceptor doping in the grain and grain boundary of a polycristalline semiconducting c eramics," *Journal of Material Research,* vol. 7, no. 12, pp. 3280-3295, 1992.
12. B. Wang, Z. Fang, Z. Fu, and Y. Peng, "Electrical Behavior against Current Impulse in ZnO Varistor Ceramics with SiO_2 Addition," *Journal of Physics: Conference Series,* vol. 1637, no. 1, 2020. https://doi.org/10.1088/1742-6596/1637/1/012026
13. J. Sun, B. Luo, and H. Li, "A Review on the Conventional Capacitors, Supercapacitors, and Emerging Hybrid Ion Capacitors: Past, Present, and Future," *Advanced Energy and Sustainability Research,* vol. 3, no. 6, 2022. https://doi.org/10.1002/aesr.202100191
14. J. He, C. Cheng, and J. Hu, "Electrical degradation of double-Schottky barrier in ZnO varistors," *AIP Advances,* vol. 6, no. 3, 2016. https://doi.org/10.1063/1.4944485
15. T. K. Gupta and W. G. Carlson, "A grain-boundary defect model for stability/instability of a ZnO varistor," *Journal of Materials Science,* vol. 20, pp. 3487-3500, 1985.
16. Y. Huang, M. Guo, and J. Li, "Multiscale defect responses in understanding degradation in zinc oxide varistor ceramics," *Ceramics International,* vol. 46, no. 14, pp. 22134-22139, 2020. https://doi.org/10.1016/j.ceramint.2020.05.286
17. H. Bai *et al.*, "Influence of SiO_2 on electrical properties of the highly nonlinear ZnO-Bi_2O_3-MnO_2 varistors," *Journal of the European Ceramic Society,* vol. 37, no. 13, pp. 3965-3971, 2017. https://doi.org/10.1016/j.jeurceramsoc.2017.05.014
18. Z. H. Wu, J. H. Fang, D. Xu, Q. D. Zhong, and L.-y. Shi, "Effect of SiO_2 addition on the microstructure and electrical properties of ZnO-based varistors," *International Journal of Minerals, Metallurgy, and Materials,* vol. 17, no. 1, pp. 86-91, 2010. https://doi.org/10.1007/s12613-010-0115-0
19. W. Long, J. Hu, J. Liu, J. He, and R. Zong, "The Effect of Aluminum on Electrical Properties of ZnO Varistors," *Journal of the American Ceramic Society,* vol. 93, no. 9, pp. 2441-2444, 2010. https://doi.org/10.1111/j.1551-2916.2010.03787.x
20. Q. Fu, C. Ke, Y. Hu, Z. Zheng, T. Chen, and Y. Xu, "Al-doped ZnO varistors prepared by a two-step doping process," *Advances in Applied Ceramics,* vol. 117, no. 4, pp. 237-242, 2018. https://doi.org/10.1080/17436753.2017.1405556
21. M. Houabes, S. Bernik, C. Talhi, and A. Bui, "The effect of aluminium oxide on the residual voltage of ZnO varistors," *Ceramics International,* vol. 31, no. 6, pp. 783-789, 2005. https://doi.org/10.1016/j.ceramint.2004.09.004
22 S. Bernik and N. Daneu, "Characteristics of .ZnO-based varistor ceramics doped with Al_2O_3," *Journal of the European Ceramic Society,* vol. 27, no. 10, pp. 3161-3170, 2007. https://doi.org/10.1016/j.jeurceramsoc.2007.02.176
23. M. Peiteado, Y. Iglesias, and A. C. Caballero, "Sodium impurities in ZnO–Bi_2O_3–Sb_2O_3 based varistors," *Ceramics International,* vol. 37, no. 3, pp. 819-824, 2011. https://doi.org/10.1016/j.ceramint.2010.10.016
24. E. L. Tikhomirova, O. G. Gromov, and Y. A. Savel'ev, "Effect of Impurities on Varistor Properties of High-Voltage ZnO Ceramics," *Russian Journal of Applied Chemistry,* vol. 94, no. 4, pp. 437-441, 2021. https://doi.org/10.1134/s1070427221040029
25. A. Smith, G. Gasgnier, and P. Abelard, "Voltage-Current Characteristics of ZnO varistors of a Simple Zinc Oxide Varistor Containing Magnesia," *Journal of the American Ceramic Society,* vol. 73, no. 4, pp. 1098-1099, 1990.
26. K. Hembram, T. N. Rao, M. Ramakrishana, R. S. Srinivasa, and A. R. Kulkarni, "Influence of CaO doping on phase, microstructure, electrical and dielectric properties of ZnO varistors," *Journal of Alloys and Compounds,* vol. 817, 2020. https://doi.org/10.1016/j.jallcom.2019.152700
27. H. Wang, H. Zhao, W. Liang, S. Fan, and J. Kang, "Effect of sintering process on the electrical properties and microstructure of Ca-doped ZnO varistor ceramics," *Materials Science in Semiconductor Processing,* vol. 133, 2021. https://doi.org/10.1016/j.mssp.2021.105880
28. H. Zhao, H. Wang, X. Meng, J. Zhao, and Q. Xie, "A method to reduce ZnO grain resistance and improve the intergranular layer resistance by Ca^{2+} and Al^{3+} co-doping," *Materials Science in Semiconductor Processing,* vol. 128, 2021. https://doi.org/10.1016/j.mssp.2021.105768
29. W. Deng, Z. Q. Lei, J. L. Zhao, Y. Q. Lu, and D. K. Xiong, "Effect of Fe_2O_3 Dopant on Electronic Densities and Electrical Properties of ZnO-Based Varistors," *Advanced Materials Research,* vol. 415-417, pp. 1042-1045, 2011. https://doi.org/10.4028/www.scientific.net/AMR.415-417.1042
30. M. Peiteado, A. M. Cruz, Y. Reyes, J. De Frutos, D. G. Calatayud, and T. Jardiel, "Progressive degradation of high voltage ZnO commercial varistors upon Fe_2O_3 doping," *Ceramics International,* vol. 40, no. 8, pp. 13395-13400, 2014. https://doi.org/10.1016/j.ceramint.2014.05.057
31. J. Shen *et al.*, "Effects of Fe and Al co-doping on the leakage current density and clamp voltage ratio of ZnO varistor," *Journal of Alloys and Compounds,* vol. 747, pp. 1018-1026, 2018. https://doi.org/10.1016/j.jallcom.2018.03.106

32. Z. Peng *et al.*, "Influence of Fe_2O_3 doping on microstructural and electrical properties of ZnO–Pr6O11 based varistor ceramic materials," *Journal of Alloys and Compounds,* vol. 508, no. 2, pp. 494-499, 2010.
https://doi.org/10.1016/j.jallcom.2010.08.100

Arrived: 29. 09. 2022
Accepted: 09. 11. 2022